PERMANENT MAGNETS

```
      IF(HY.LT.0.0) T(1,J)=270.0
    3 HM(1,J)=ABS(HY)
      DO 4 I=1,IN
      T(I,1)=270.0
    4 HM(1,1)=HM(I,2)
      T(IN,1)=0.0
      RETURN
      END
```

PERMANENT MAGNETS RESULTS

```
REGION SIZE= 9X10
MAGNET SIZE= 4X 5
MESH INTERVAL= 0.10
MAGNETIZATION= 5.00
CONVERGENCE FACTOR= 1.50

     MESH USED

 . . . . . .
 . . . . . .
 . . . . . .
 . . . . . .
 . . . . . .
 1 1 1 1 . . . . .
 1 1 1 1 . . . . .
 1 1 1 1 . . . . .
 1 1 1 1 . . . . .
 1 1 1 1 . . . . .

 NO OF ITERATIONS = 28  REMAX= 0.2361E-03     RESUM=0.9454E-04
```

MAGNETOSTATIC POTENTIAL

0.00	0.00	0.00	0.00	0.00	0.00	0.00	0.00	0.00
0.14	0.14	0.13	0.11	0.08	0.06	0.04	0.02	0.00
0.30	0.29	0.26	0.22	0.17	0.12	0.08	0.04	0.00
0.47	0.45	0.41	0.34	0.26	0.18	0.11	0.05	0.00
0.66	0.65	0.59	0.48	0.33	0.22	0.13	0.06	0.00
0.90	0.88	0.82	0.65	0.38	0.23	0.14	0.06	0.00
0.63	0.61	0.55	0.43	0.30	0.20	0.12	0.06	0.00
0.40	0.38	0.34	0.27	0.21	0.14	0.09	0.04	0.00
0.19	0.19	0.17	0.13	0.10	0.07	0.05	0.02	0.00
0.00	0.00	0.00	0.00	0.00	0.00	0.00	0.00	0.00

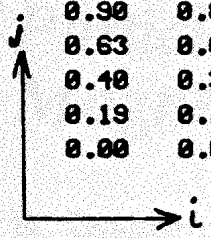

MAGNETIC FIELD DIRECTIONS

90.00	89.59	89.55	89.47	89.33	89.07	88.54	86.99	0.00
90.00	88.36	84.74	80.29	74.81	68.41	59.39	41.49	0.00
90.00	86.96	80.14	71.18	59.51	48.09	36.15	20.81	0.00
90.00	85.96	76.82	63.07	42.18	28.34	18.73	9.87	0.00
90.00	85.63	76.12	57.47	17.95	7.57	3.70	1.62	0.00
270.00	273.85	282.27	306.79	344.04	346.72	349.77	354.07	0.00
270.00	274.63	286.28	309.11	321.70	330.51	337.35	346.67	0.00
270.00	273.77	282.85	296.28	304.04	313.13	322.43	336.79	0.00
270.00	272.02	276.75	283.16	286.97	293.02	300.97	317.54	0.00
270.00	270.00	270.00	270.00	270.00	270.00	270.00	270.00	0.00

MAGNETIC FIELD MAGNITUDES

1.44	1.40	1.27	1.08	0.85	0.61	0.39	0.19	0.01
1.52	1.48	1.35	1.14	0.89	0.64	0.43	0.27	0.19
1.70	1.65	1.52	1.28	0.98	0.74	0.55	0.42	0.37
1.97	1.93	1.82	1.54	1.16	0.90	0.71	0.58	0.52
2.32	2.33	2.38	2.05	1.53	1.15	0.87	0.70	0.62
2.68	2.68	2.76	2.81	2.82	1.50	0.98	0.74	0.64
2.31	2.27	2.15	1.96	1.57	1.19	0.86	0.65	0.56
2.05	1.99	1.82	1.56	1.23	0.94	0.68	0.50	0.41
1.92	1.86	1.67	1.38	1.08	0.79	0.53	0.32	0.22
1.92	1.86	1.67	1.38	1.08	0.79	0.53	0.32	0.22

Physics Programs
Edited by A. D. Boardman

CHAPTER 5

Particle Capture in High Gradient Magnetic Separation

R. GERBER

1. INTRODUCTION

High gradient magnetic separation (HGMS) is a technique for the removal of weakly magnetic particles from suspensions that has many practical applications such as sewage and water treatments and the processing of industrial slurries. The method is based on the utilization of a magnetic traction force which extracts the particles from the fluid when the suspension passes through the separator system. The magnetic traction force, $\mathbf{F}_m$, is proportional to the difference, $\chi_p - \chi_f$, between the particle and fluid susceptibilities and, since curl $\mathbf{H} = 0$, to the product, H grad H, of the magnitude of the magnetic field and its gradient at the position of the particle. The difference $\chi_p - \chi_f$ is usually very small for weakly magnetic particles, and also the magnetic field magnitude H cannot be increased above a certain upper limit for technical reasons. Thus an efficient extraction, which results from a large value of $\mathbf{F}_m$, requires that the value of grad H be high. Hence the name of the method.

An example of a HGMS system is shown schematically in Figure 1. It consists of a canister, filled with an ordered matrix of very thin magnetic wires, which is placed in a magnetic field, large enough to saturate the wires. The canister, using an appropriate plumbing, conducts either the suspension of mixed magnetic and non-magnetic particles or flush water through the system. The thin wires of the matrix dehomogenize the background magnetic field and give rise to a high value of its gradient in their immediate surroundings. When the magnetic field is on, the suspension of particles to be separated flows through the matrix, the magnetic particles are captured on to the wires, and the purified suspension leaves the system. At intervals, when the retention capacity of the matrix is reached, the feed is halted, the magnetic field is switched off, and the magnetic particles are flushed out of the separator. Then the cycle is repeated.

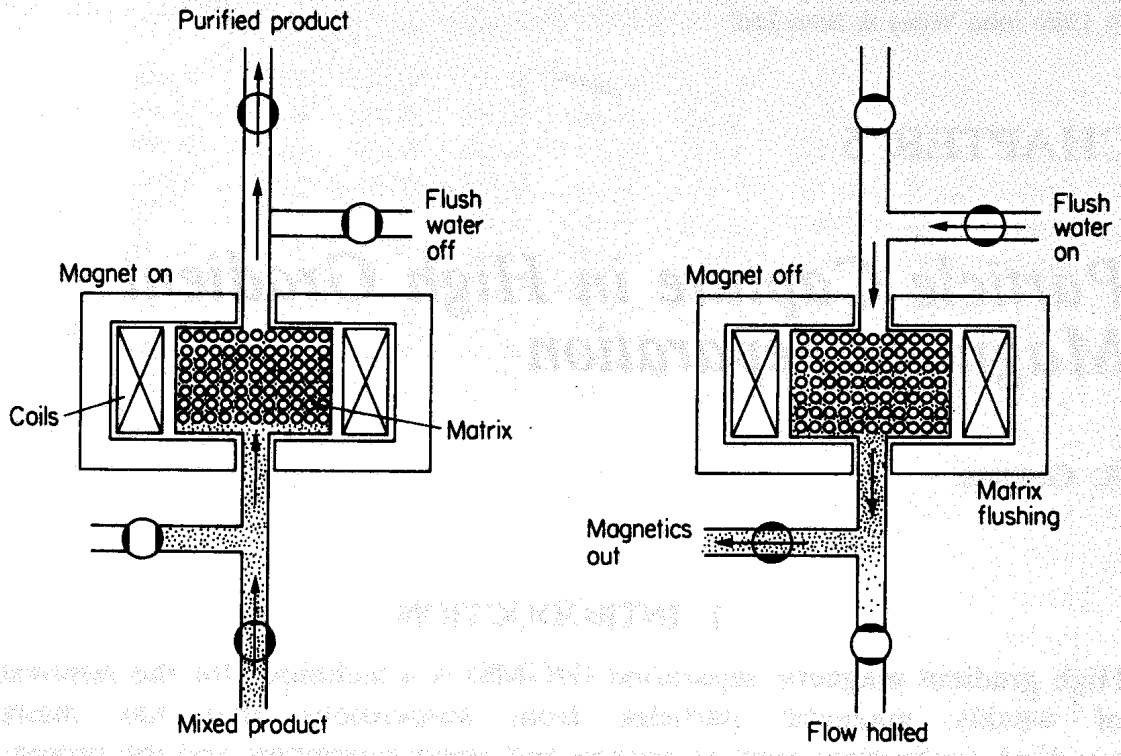

Figure 1. Schematic view of a high gradient magnetic separator

The packing fraction, F (which is defined as the volume occupied by the wires to that of the canister), of the matrix is typically between 0.05 and 0.1. Thus most of the space in the canister is actually free. This has two important consequences. First, the fluid impedance of the system is low. Hence a large amount of material can be passed through and treated by the separator in a short period of time. Second, the capture process can be considered in a single-wire approximation.[1] In this approximation, since the wires in the canister are relatively far apart, it is assumed that the particles interact with only one individual wire at a time.

An important quantity characterizing any separation system is the filter performance. It is given as the ratio N_{out}/N_{in}, where N_{out} and N_{in} are the number of magnetic particles leaving and entering the separator, respectively. The smaller the ratio the better the performance.

In order to obtain some idea of filter performance let us consider an ordered matrix comprised of a large number of stacked-up sheets of gauze which are woven in a regular rectangular pattern from a thin ferromagnetic wire of radius a. If the magnetic field is normal to the surface of each sheet and if certain limiting conditions are fulfilled, it can be shown[2] that the filter performance is given by the formula

$$N_{out} = \exp\left(\frac{-2R_{ca}FL}{\pi a}\right)N_{in}, \tag{1}$$

where L is the total length of the matrix stack and R_{ca} is the capture radius (in units of a) associated with an individual wire.

It is clear that particle trajectories and capture radii are of fundamental importance for HGMS. A useful starting point for an investigation of this technique is a computational study dealing with particle capture in the single-wire approximation, and this is presented in this chapter.

2. SINGLE-WIRE APPROXIMATION

2.1 Configuration

The background magnetic field in the separator becomes inhomogeneous due to the appearance of magnetic charges on the ferromagnetic wires of the matrix. This effect is a maximum if the ordered matrix is arranged so that the direction of the field is always perpendicular to the axes of the wires. Therefore, in the single-wire approximation, we consider a configuration as shown in Figure 2. A ferromagnetic wire of radius a, saturation magnetization M_s, is placed axially along the z-axis of an orthogonal coordinate system. A magnetic field, H_0, sufficient to saturate the wire, is applied in the x-direction and a fluid of viscosity η flows with a background velocity V_0 along a direction which lies in the xy plane making an angle α with the x-axis.

A completely arbitrary direction of fluid flow is perfectly possible in

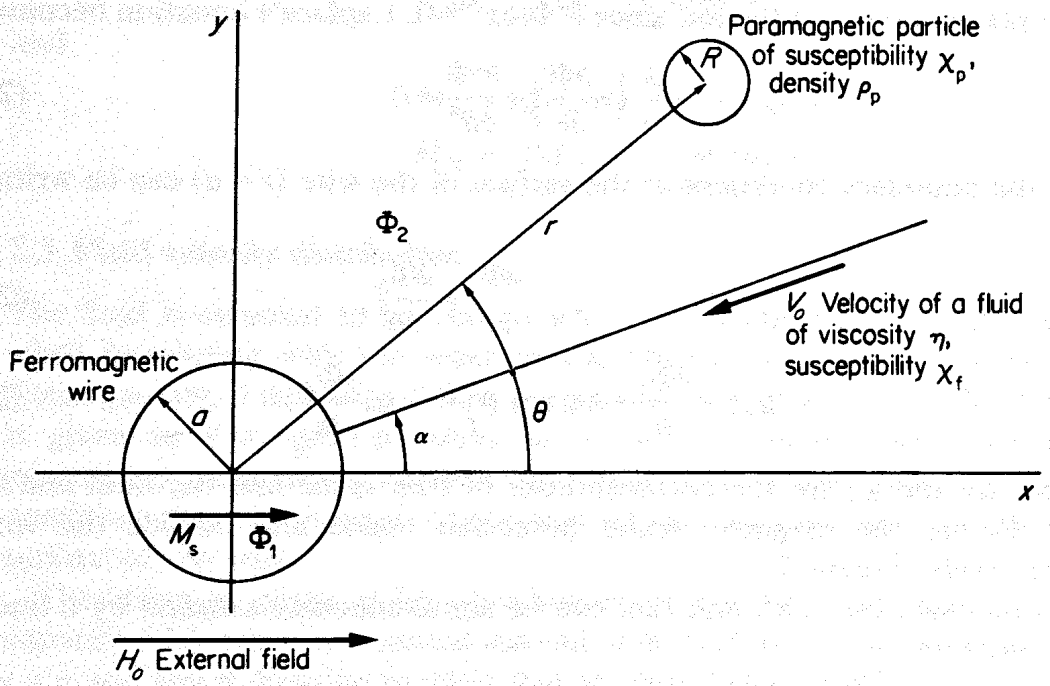

Figure 2. Configuration of the particle capture problem in the single-wire approximation

HGMS. However, such direction can be resolved in one lying in the xy plane and in one parallel with the z-axis. The latter case, the so-called axial configuration, can be solved analytically[3] and is therefore outside the scope of this chapter.

Paramagnetic particles of spherical shape with radius $R(R \ll a)$, volume V_p, susceptibility χ_p and density ρ_p, are carried by the fluid. The flow of the fluid around the wire is considered to be streamlined and frictionless, but the particles are assumed to experience a viscous drag force $\mathbf{F}_v$ given by the Stokes equation $\mathbf{F}_v = -6\pi\eta R(\mathbf{v}-\mathbf{V})$, where $(\mathbf{v}-\mathbf{V})$ is the relative velocity of the particle with respect to the fluid.

Physical quantities used throughout this chapter are in SI units (Sommerfeld system). The metric part of their dimensions may be sometimes expressed in terms of the wire radius a. Then, to indicate this renormalization, the symbols are provided with the subscript a e.g. $R_a = R/a$, $V_{pa} = V_p/a^3$, etc.).

2.2 Magnetic field

The magnetic field $\mathbf{H}$ of a wire magnetized by a uniform background field $\mathbf{H}_0$ can be expressed as $\mathbf{H} = -\text{grad}\,\Phi$, where Φ is the magnetic scalar potential. Since $\text{div}\,\mathbf{B} = 0$, we can write for a linear medium $\text{div}\,\mathbf{B} = \text{div}\,(\mu\mathbf{H}) = \mu\,\text{div}\,\mathbf{H} = \mu\,\text{div grad}\,\Phi = 0$. Thus the potential Φ must satisfy Laplace's equation $\nabla^2\Phi = 0$ and also the boundary conditions requiring the tangential components of $\mathbf{H}$ and the normal components of $\mathbf{B}$ to be continuous at the surface of the wire.

In plane polar coordinates, since $\partial^2\Phi/\partial z^2 = 0$, Laplace's equation becomes

$$r\frac{\partial}{\partial r}\left(r\frac{\partial\Phi}{\partial r}\right)+\frac{\partial^2\Phi}{\partial\theta^2}=0 \tag{2a}$$

and the boundary conditions at the surface of the wire ($r = a$) can be written as

$$\frac{\partial\Phi_1}{\partial\theta}=\frac{\partial\Phi_2}{\partial\theta}, \tag{2b}$$

$$\mu_0\left(-\frac{\partial\Phi_1}{\partial r}+M_s\cos\theta\right)=-\mu_f\frac{\partial\Phi_2}{\partial r}, \tag{2c}$$

where μ_0 and μ_f are the permeabilities of free space and the fluid and Φ_1 and Φ_2 are the magnetic scalar potentials inside and outside the wire, respectively (Figure 2).

Equations (2a), (2b), and (2c) can be simultaneously satisfied by a linear combination

$$\Phi_1 = -C_1 r\cos\theta + A_1 r^{-1}\cos\theta, \tag{3a}$$

$$\Phi_2 = -C_2 r\cos\theta + A_2 r^{-1}\cos\theta \tag{3b}$$

of cylindrical harmonics.[4]

The field in the origin (on the wire axis) is finite, hence $A_1 = 0$. At large distances, the field tends to H_0, consequently $C_2 = H_0$. The remaining two constants, C_1 and A_2, are obtained by substitution of equations (3a, b) into (2b, c). We obtain

$$C_1 = H_0 - A_2 a^{-2} \tag{4}$$

and

$$A_2 = \frac{\mu_0 - \mu_f}{\mu_0 + \mu_f} H_0 a^2 + \frac{\mu_0}{\mu_0 + \mu_f} M_s a^2. \tag{5}$$

Since for most practical cases $|\mu_0 - \mu_f| \lesssim 10^{-3}$, the first term in equation (5) can be neglected in comparison with the second. Thus we obtain from (4) and (5)

$$A_2 = \tfrac{1}{2} M_s a^2, \tag{6}$$

$$C_1 = H_0 - \tfrac{1}{2} M_s. \tag{7}$$

Substituting $A_1 = 0$, $C_2 = H_0$, equations (6) and (7) into (3a, b) we obtain the scalar potentials, the negative gradient of which gives the respective magnetic fields, $\mathbf{H}_1$ and $\mathbf{H}_2$, inside and outside the wire. Their components are

$$H_{1r} = (H_0 - \tfrac{1}{2} M_s)\cos\theta, \tag{8a}$$

$$H_{1\theta} = -(H_0 - \tfrac{1}{2} M_s)\sin\theta, \tag{8b}$$

and

$$H_{2r} = (\tfrac{1}{2} M_s a^2 r^{-2} + H_0)\cos\theta, \tag{9a}$$

$$H_{2\theta} = (\tfrac{1}{2} M_s a^2 r^{-2} - H_0)\sin\theta. \tag{9b}$$

2.3 Fluid velocity distribution

The fluid is assumed to be viscous when interacting with the particles, but when interacting with the wires of the filter it is considered to be ideal. Consequently, if irrotational flow is assumed, the velocity of the fluid motion is given as $\mathbf{V} = -\text{grad}\,\psi$, where ψ is the velocity potential. Again, the potential ψ must satisfy Laplace's equation $\nabla^2\psi = 0$ and also the boundary condition that the normal component of the velocity must vanish at the surface of the wire.

Therefore, in plane polar coordinates, ψ has to satisfy simultaneously equation (2a), when substituted instead of Φ, and the condition $\partial\psi/\partial r = 0$ for $r = a$ and any θ. Bearing in mind that at large distances the flow takes place at an angle α with a uniform velocity V_0, we can see immediately that the function

$$\psi = -V_0 r\cos(\theta - \alpha) + A r^{-1}\cos(\theta - \alpha), \tag{10}$$

which is analogous to (3a, b), will satisfy both equation (2a) and the boundary condition. Substitution of (10) into $(\partial\psi/\partial r)_{r=a}=0$ gives $A=-V_0a^2$. This value can now be used in (10), when the negative gradient is taken of this expression. Thus we obtain the components of the fluid velocity:

$$V_r = V_0(1-a^2r^{-2})\cos(\theta-\alpha), \tag{11a}$$

$$V_\theta = -V_0(1+a^2r^{-2})\sin(\theta-\alpha). \tag{11b}$$

2.4 Equations of particle motion

The equation of motion can be written in a vector form as

$$m\mathbf{a}=\mathbf{F}_v+\mathbf{F}_m, \tag{12}$$

where $m=\frac{4}{3}\pi R^3\rho_p$ is the mass of the particle, $\mathbf{a}$ is the acceleration, $\mathbf{F}_v$ and $\mathbf{F}_m$ are the viscous drag and magnetic traction force, respectively. In order to be able to solve equation (12) we need to establish the components of all its terms in plane polar coordinates r and θ.

Consider two mutually perpendicular unit vectors $\hat{\mathbf{r}}$ and $\hat{\boldsymbol{\theta}}$ which have directions of increasing $\mathbf{r}$ and increasing θ. Their directions change with time and since the derivative of a unit vector is perpendicular to the vector, we have

$$\frac{\mathrm{d}\hat{\mathbf{r}}}{\mathrm{d}t}=\frac{\mathrm{d}\theta}{\mathrm{d}t}\hat{\boldsymbol{\theta}}, \tag{13a}$$

$$\frac{\mathrm{d}\hat{\boldsymbol{\theta}}}{\mathrm{d}t}=-\frac{\mathrm{d}\theta}{\mathrm{d}t}\hat{\mathbf{r}}. \tag{13b}$$

Now, the position of the particle in plane polar coordinates is given by $\mathbf{r}=r\hat{\mathbf{r}}$. Differentiating this equation and using (13a, b), we obtain the particle velocity $\mathbf{v}$, the components of which are $v_r=\mathrm{d}r/\mathrm{d}t$ and $v_\theta=r(\mathrm{d}\theta/\mathrm{d}t)$. By second differentiation, we obtain the particle acceleration $\mathbf{a}$ and its components

$$a_r=\frac{\mathrm{d}^2r}{\mathrm{d}t^2}-r\left(\frac{\mathrm{d}\theta}{\mathrm{d}t}\right)^2, \tag{14a}$$

$$a_\theta=r\frac{\mathrm{d}^2\theta}{\mathrm{d}t^2}+2\frac{dr}{\mathrm{d}t}\frac{\mathrm{d}\theta}{\mathrm{d}t}. \tag{14b}$$

The components of the viscous drag force $\mathbf{F}_v$ are

$$F_{vr}=-6\pi\eta R\left(\frac{\mathrm{d}r}{\mathrm{d}t}-V_r\right) \tag{15a}$$

and

$$F_{v\theta} = -6\pi\eta R\left(r\frac{d\theta}{dt} - V_\theta\right), \tag{15b}$$

where V_r and V_θ are given by equations (11a, b).

To establish the components of the magnetic traction force $\mathbf{F}_m$ we have to consider first the magnetic energy of a system comprising a fluid and a particle.

The magnetic energy density is expressed in general as $\frac{1}{2}HB$. Imagine a volume V_p demarcated inside the fluid. The magnetic energy of the fluid enclosed in this volume is $\frac{1}{2}HB_f V_p = \frac{1}{2}\mu_f V_p H^2$. Let us now remove the fluid from the volume V_p and replace it by the particle. The energy associated with the particle itself is $\frac{1}{2}\mu_p V_p H^2$. The energy increment U of the system (particle + fluid) is given as the difference between these two energies, i.e. $U = \frac{1}{2}(\mu_p - \mu_f)V_p H^2$. Taking ∇U (positive gradient, since the magnetic energy is of the same nature as the kinetic energy) we get

$$\mathbf{F}_m = \tfrac{1}{2}\mu_0 \chi V_p \nabla(H^2), \tag{16}$$

where $\chi = \chi_p - \chi_f$ is the difference between susceptibilities of the particle and the fluid.

Considering a spherical particle, $V_p = \frac{4}{3}\pi R^3$, and substituting $H^2 = H_{2r}^2 + H_{2\theta}^2$ from (9a, b) into (16), we obtain, after some manipulation, the components of the magnetic traction force

$$F_{mr} = -\frac{4\pi\mu_0\chi M_s a^2 R^3}{3r^3}\left(\frac{M_s a^2}{2r^2} + H_0\cos 2\theta\right), \tag{17a}$$

$$F_{m\theta} = -\frac{4\pi\mu_0\chi M_s a^2 R^3}{3r^3} H_0 \sin 2\theta. \tag{17b}$$

Combining equations (14a, b), (15a, b), and (17a, b) with (12) we obtain the complete equations of motion: in radial direction

$$\frac{2\rho_p R^2}{9\eta}\left(\frac{d^2 r_a}{dt^2} - r_a\left(\frac{d\theta}{dt}\right)^2\right) + \frac{dr_a}{dt} = V_{0a}\left(1 - \frac{1}{r_a^2}\right)\cos(\theta - \alpha) - V_{ma}\left(\frac{M_s}{2H_0 r_a^2} + \cos 2\theta\right)\frac{1}{r_a^3} \tag{18a}$$

and in aximuthal direction

$$\frac{2\rho_p R^2}{9\eta}\left(r_a\frac{d^2\theta}{dt^2} + 2\frac{dr_a}{dt}\frac{d\theta}{dt}\right) + r_a\frac{d\theta}{dt} = -V_{0a}\left(1 + \frac{1}{r_a^2}\right)\sin(\theta - \alpha) - V_{ma}\frac{\sin 2\theta}{r_a^3}, \tag{18b}$$

where $r_a = r/a$, $V_{0a} = V_0/a$, $V_{ma} = V_m/a = \frac{2}{9}(\chi\mu_0 M_s H_0 R_a^2/\eta)$ and $R_a = R/a$. The quantity V_m, the dimensions of which are m s^{-1}, is called the magnetic velocity.

The first (inertial) terms in equations (18a, b) can usually be neglected in comparison with others in case of HGMS of small particles in liquids. Then R^2 is very small and η moderately high and (18a, b) reduce to a pair of first-order differential equations:

$$\frac{dr_a}{dt} = V_{0a}\left(1 - \frac{1}{r_a^2}\right)\cos(\theta - \alpha) - V_{ma}\left(\frac{K}{r_a^2} + \cos 2\theta\right)\frac{1}{r_a^3}, \tag{19a}$$

$$\frac{d\theta}{dt} = -V_{0a}\left(1 + \frac{1}{r_a^2}\right)\frac{\sin(\theta - \alpha)}{r_a} - V_{ma}\frac{\sin 2\theta}{r_a^4}, \tag{19b}$$

where $K = M_s/2H_0$. Equations (19a, b) will be analysed and numerically solved in the main text of this chapter.

If the particle bearing fluid is a gas, η is rather small and the inertial term cannot be neglected. Complete equations of motion are therefore required for a numerical solution of this problem.[5] An appropriate extension of our computer programs to perform this task also is included in the suggested exercises.

3. NUMERICAL SOLUTION OF ORDINARY DIFFERENTIAL EQUATIONS

3.1 Predictor–corrector method

Consider a first-order initial-value problem

$$y' = f(x, y), \tag{20a}$$

$$y(x_0) = y_0, \tag{20b}$$

where x_0, y_0, and the function $f(x, y)$ are given, y' denotes dy/dx. Under quite general conditions this problem has a unique solution $y(x)$ in the interval[6] $\langle x_0, \bar{x}\rangle$, $\bar{x} \neq x_0$.

We would like to find a numerical approximation to the solution $y(x)$. Let us divide the interval $\langle x_0, \bar{x}\rangle$ into m subintervals, each of length h. Thus, there are $m+1$ points

$$x_n = x_0 + nh, \qquad n = 0, 1, 2, \ldots, m,$$

where we are seeking the values $y_1, y_2, \ldots, y_m$ of the solution $y(x)$.

The numerical method of solving differential equations such as (20a, b) involves the procedure which yields y_{n+1}, given the sequence $y_n, y_{n-1}, y_{n-2} \ldots$ up to y_{n-s}. The value of s may be 0, 1, 2, etc. When y_{n+1} is found, the procedure is repeated until the whole interval $\langle x_0, \bar{x}\rangle$ is covered.

The Euler method, which has $s = 0$, is the simplest numerical method for solving initial-value problems of the type (20a, b). To derive this method, assume that the value y_n is known and integrate (20a) from x_n to x_{n+1}. We get

$$y_{n+1} - y_n = \int_{x_n}^{x_{n+1}} f(x, y(x))\, dx. \tag{21}$$

The integral in (21) can be approximated by the rectangle rule as $hf(x_n, y(x_n))$. Thus we obtain the formula (procedure)

$$y_{n+1} - y_n = hf(x_n, y_n). \tag{22}$$

Starting with $n = 0$, i.e. substituting first the known value y_0, we find by repetition all required values.

Evidently, the accuracy of determination of y_{n+1} depends on h. It can be shown that the single step (quadrature) error is approximately proportional to h^2 for the Euler method. We can, therefore, increase the accuracy by decreasing the size of h. This will, however, increase the number of steps and hence the computing time. Moreover, with each step an accumulated error will enter into the process. This error will partly offset the improvement in accuracy which was gained by the reduction of h. Clearly, one would like to increase the accuracy without the need to reduce h. This can be achieved by using numerical quadrature formulae, based on Lagrangian interpolation, for the approximation of the integral in equation (21). These quadrature formulae take into account the behaviour of the function $f(x, y(x))$ in a wider surroundings of the interval of integration.Thus the integral in (21) can be expressed to a high degree of accuracy for a relatively large h.

We have two types of formulae available. The open or predictor formula

$$y_{n+1} - y_{n+1-q} = h \sum_{i=1}^{M} \beta_i f(x_{n+1-i}, y_{n+1-i}), \tag{23a}$$

and the closed or corrector formula

$$y_{n+1} - y_{n+1-q} = h \sum_{i=0}^{M'} \beta_i' f(x_{n+1-i}, y_{n+1-i}), \tag{23b}$$

where q is a fixed integer, and β_i and β_i' are the numerical coefficients. A full analysis and values of q, β_i, and β_i' of various methods can be found in Young and Gregory.[6]

Note that equation (23a) contains y_{n+1} explicitly, whereas (23b) contains y_{n+1} implicitly, hence the names 'open' and 'closed' formula, respectively.

Formulae (23a, b) together form the predictor–corrector method. It works as follows: let us assume that we are at the nth point and that we already know, by some means, the values $y_n, y_{n-1}, \ldots, y_{n-M+1}$. Substituting these known values in (23a) we obtain the predicted value $y^{(P)}$. Substituting $y^{(P)}_{n+1}$ together with $y_n, y_{n-1}, \ldots$ etc. in (23b) we obtain the corrected value $y^{(C)}_{n+1}$. If $|(y^{(P)}_{n+1} - y^{(C)}_{n+1})/y^{(C)}_{n+1}| < E$, where E is the stipulated error, we put $y_{n+1} = y^{(C)}_{n+1}$ and repeat the cycle for the next point, i.e. for $n+1$. If the relative error between the predicted and corrected value is larger than E we have to reduce h and calculate the next $M-1$ values by some other means (see section 3.2) before the predictor–corrector method can again be employed.

There is a large family of predictor–corrector methods available. The Adams–Moulton method, which is employed in our program, is particularly attractive, since it is of a good stability and high precision (quadrature error $\simeq 0(h^5)$). The numerical quantities characterizing this method are $q = 1$, $M = 4$, $\beta_i = 55/24$, $-59/24$, $37/24$, $-9/24$, $M' = 3$, $\beta'_i = 9/24$, $19/24$, $-5/24$, $1/24$.

3.2 Runge–Kutta method

To get a predictor–corrector method into action we need to know the values of y at several starting points $x_0 + h, x_0 + 2h, \ldots, x_0 + sh$, in addition to the given value of $y(x_0)$. Hence the desire for an accurate self-starting method, i.e. a high order method which would require a knowledge of y at only one initial point. The Runge–Kutta method is of this type and its derivation will be briefly described here. Consider again equation (21). We can write

$$y^{(P)}_{n+1} = y_n + hf(x_n, y_n), \tag{24a}$$

$$y_{n+1} = y_n + \frac{h}{2}[f(x_n, y_n) + f(x_{n+1}, y^{(P)}_{n+1})], \tag{24b}$$

where the predicted value $y^{(P)}_{n+1}$ and the corrected value y_{n+1} were obtained by applying the rectangle and the trapezoidal rule, respectively. Formulae (24a, b), which constitute the Heun predictor–corrector method, can be rewritten in the following form:

$$y_{n+1} = y_n + \alpha_1 \Delta_1 + \alpha_2 \Delta_2, \tag{25}$$

where

$$\Delta_1 = hf(x_n, y_n), \tag{26a}$$

$$\Delta_2 = hf(x_n + \rho h, y_n + \rho \Delta_1), \tag{26b}$$

and where the numerical coefficients have the values of $\rho = 1$, $\alpha_1 = \frac{1}{2}$, $\alpha_2 = \frac{1}{2}$.

Thus instead of two formúlae, (24a, b), we have one formula, (25), with two 'differential' increments Δ_1 and Δ_2. The first increment Δ_1 serves not only in (25) but also as a 'predictor' for the second increment Δ_2 in (26b).

Generalizing formulae (25) and (26a, b) to involve four increments and determining the appropriate numerical coefficients by comparison of $y_{n+1} = \sum_{j=1}^{4} \alpha_j \Delta_j$ with y_{n+1} given as a Taylor's series expansion of $y(x)$ at x_n, we obtain the (fourth-order) Runge–Kutta method as

$$y_{n+1} = y_n + \tfrac{1}{6}(\Delta_1 + 2\Delta_2 + 2\Delta_3 + \Delta_4), \tag{27}$$

where

$$\Delta_1 = hf(x_n, y_n), \tag{28a}$$

$$\Delta_2 = hf(x_n + \tfrac{1}{2}h, y_n + \tfrac{1}{2}\Delta_1), \tag{28b}$$

$$\Delta_3 = hf(x_n + \tfrac{1}{2}h, y_n + \tfrac{1}{2}\Delta_2), \tag{28c}$$

$$\Delta_4 = hf(x_n + h, y_n + \Delta_3). \tag{28d}$$

The Runge–Kutta method, the single step error of which is $0(h^5)$, is used in our programs either in its own right or in connection with the Adams–Moulton method as a starter. This choice satisfies the rule that the starter should have approximately the same accuracy as the main execution method.

3.3 Systems of equations and higher order equations

Many physical problems involve coupled differential equations such as (18a, b) and (19a, b). Consequently, it is necessary to develop a method of solving them. Consider a first-order system

$$\begin{aligned} y_1'(x) &= f_1(x, y_1, y_2, \ldots, y_n), \\ y_2'(x) &= f_2(x, y_1, y_2, \ldots, y_n), \\ &\vdots \\ y_n'(x) &= f_n(x, y_1, y_2, \ldots, y_n), \end{aligned} \tag{29a}$$

with initial conditions

$$y_1(x_0), y_2(x_0), \ldots, y_n(x_0), \tag{29b}$$

where x_0, initial conditions (29b), and the functions

$$f_j(x, y_1, y_2, \ldots, y_n), \; j = 1, 2, \ldots, n,$$

are given.

Let us introduce the vector notation:[6]

$$\mathbf{y}(x)=\begin{pmatrix} y_1(x) \\ y_2(x) \\ \cdot \\ \cdot \\ \cdot \\ y_n(x) \end{pmatrix}, \qquad \mathbf{y}'(x)=\begin{pmatrix} y_1'(x) \\ y_2'(x) \\ \cdot \\ \cdot \\ \cdot \\ y_n'(x) \end{pmatrix},$$

$$\mathbf{f}(x,\mathbf{y})=\begin{pmatrix} f_1(x, y_1, y_2, \ldots, y_n) \\ f_2(x, y_1, y_2, \ldots, y_n) \\ \cdot \\ \cdot \\ \cdot \\ f_n(x, y_1, y_2, \ldots, y_n) \end{pmatrix}=\begin{pmatrix} f_1(x,\mathbf{y}) \\ f_2(x,\mathbf{y}) \\ \cdot \\ \cdot \\ \cdot \\ f_n(x,\mathbf{y}) \end{pmatrix},$$

etc. The system (29a) and the initial conditions (29b) can then be rewritten as follows:

$$\mathbf{y}'=\mathbf{f}(x,\mathbf{y}), \tag{30a}$$

$$\mathbf{y}(x_0)=\mathbf{y}_0. \tag{30b}$$

Equations (30a, b) are of the same form as (20a, b). Consequently, the Adams–Moulton method for solution of a system of first-order differential equations can be obtained from (23a, b) if scalar quantities are replaced by vectors and the numerical coefficients β_i, β_i' are left unchanged. Thus we get

$$\mathbf{y}_{n+1}^{(P)}=\mathbf{y}_n+\frac{h}{24}(55\mathbf{f}(x_n,\mathbf{y}_n)-59\mathbf{f}(x_{n-1},\mathbf{y}_{n-1}) +37\mathbf{f}(x_{n-2},\mathbf{y}_{n-2})-9\mathbf{f}(x_{n-3},\mathbf{y}_{n-3})), \tag{31a}$$

$$\mathbf{y}_{n+1}=\mathbf{y}_n+\frac{h}{24}(9\mathbf{f}(x_{n+1},\mathbf{y}_{n+1}^{(P)})+19\mathbf{f}(x_n,\mathbf{y}_n) -5\mathbf{f}(x_{n-1},\mathbf{y}_{n-1})+\mathbf{f}(x_{n-2},\mathbf{y}_{n-2})). \tag{31b}$$

Similarly, the Runge–Kutta method is obtained from (27) and (28a, b, c, d) as

$$\mathbf{y}_{n+1}=\mathbf{y}_n+\tfrac{1}{6}(\boldsymbol{\Delta}_n^{(1)}+2\boldsymbol{\Delta}_n^{(2)}+2\boldsymbol{\Delta}_n^{(3)}+\boldsymbol{\Delta}_n^{(4)}), \tag{32}$$

where

$$\boldsymbol{\Delta}_n^{(1)}=h\mathbf{f}(x_n,\mathbf{y}_n), \tag{33a}$$

$$\boldsymbol{\Delta}_n^{(2)}=h\mathbf{f}(x_n+\tfrac{1}{2}h,\mathbf{y}_n+\tfrac{1}{2}\boldsymbol{\Delta}_n^{(1)}), \tag{33b}$$

$$\boldsymbol{\Delta}_n^{(3)}=h\mathbf{f}(x_n+\tfrac{1}{2}h,\mathbf{y}_n+\tfrac{1}{2}\boldsymbol{\Delta}_n^{(2)}), \tag{33c}$$

$$\boldsymbol{\Delta}_n^{(4)}=h\mathbf{f}(x_n+h,\mathbf{y}_n+\boldsymbol{\Delta}_n^{(3)}). \tag{33d}$$

It is easy to show that the problem of solving a single differential equation of higher order can be reduced to the problem of solving a system of first-order differential equations.

Consider

$$y^{(n)} = f(x, y, y', \ldots, y^{(n-1)}), \tag{34a}$$

where

$$y(x_0) = y_0,\ y'(x_0) = y'_0, \ldots, y^{(n-1)}(x_0) = y_0^{(n-1)} \tag{34b}$$

are the given initial conditions at the point x_0.

We can define a set of new functions as

$$y_1(x) = y(x),\ y_2(x) = y'(x), \ldots, y_n(x) = y^{(n-1)}(x).$$

It is obvious that the functions $y_1(x), y_2(x), \ldots, y_n(x)$ satisfy the system

$$\begin{aligned} y'_1 &= y_2 \\ y'_2 &= y_3 \\ &\cdot \\ &\cdot \\ &\cdot \\ y'_{n-1} &= y_n \\ y'_n &= f(x, y_1, y_2, \ldots, y_n), \end{aligned} \tag{35a}$$

and the initial conditions

$$y_1(x_0) = y_0, \qquad y_2(x_0) = y'_0, \ldots, \qquad y_n(x_0) = y_0^{(n-1)}. \tag{35b}$$

Thus by solving (35a, b) we find the function $y_1(x) = y(x)$ and its n derivative which are the solution to (34a, b).

Consequently, formulae (31a, b) or (32) and (33a, b, c, d) can also be used for finding a numerical solution of an equation of higher order if the indicated transformation to a system of first-order equations is used.

4. COMPUTER PROGRAMS

4.1 Main program

The objective of the main program is to calculate particle trajectories and capture radii R_{ca} with a prescribed accuracy for a wide variety of input parameters and initial conditions. The program consists of the MASTER section and the subroutines FUNCTN, RK, AM and XSECT.

The MASTER section handles the input–output operations and calls the relevant subroutines to perform the computation.

The input data are:

J—the control integer which selects the iterating subroutine;

K—the control integer which selects whether the output is directed to a lineprinter or/and to a file;

IO—the number of trajectories or capture radii R_{ca} to be calculated;

ALPHA—the angle α which the fluid flow makes with the external field H_0. These directions also enable us to define two convenient frames of reference, the primary has an x-axis parallel to H_0 and the secondary has an x-axis anti-parallel to the flow (Figure 3).

And

(a) if either the RK or AM subroutine has been chosen:

XAO and YAO—the starting point in the secondary frame of reference. These values are transformed in primary coordinates and

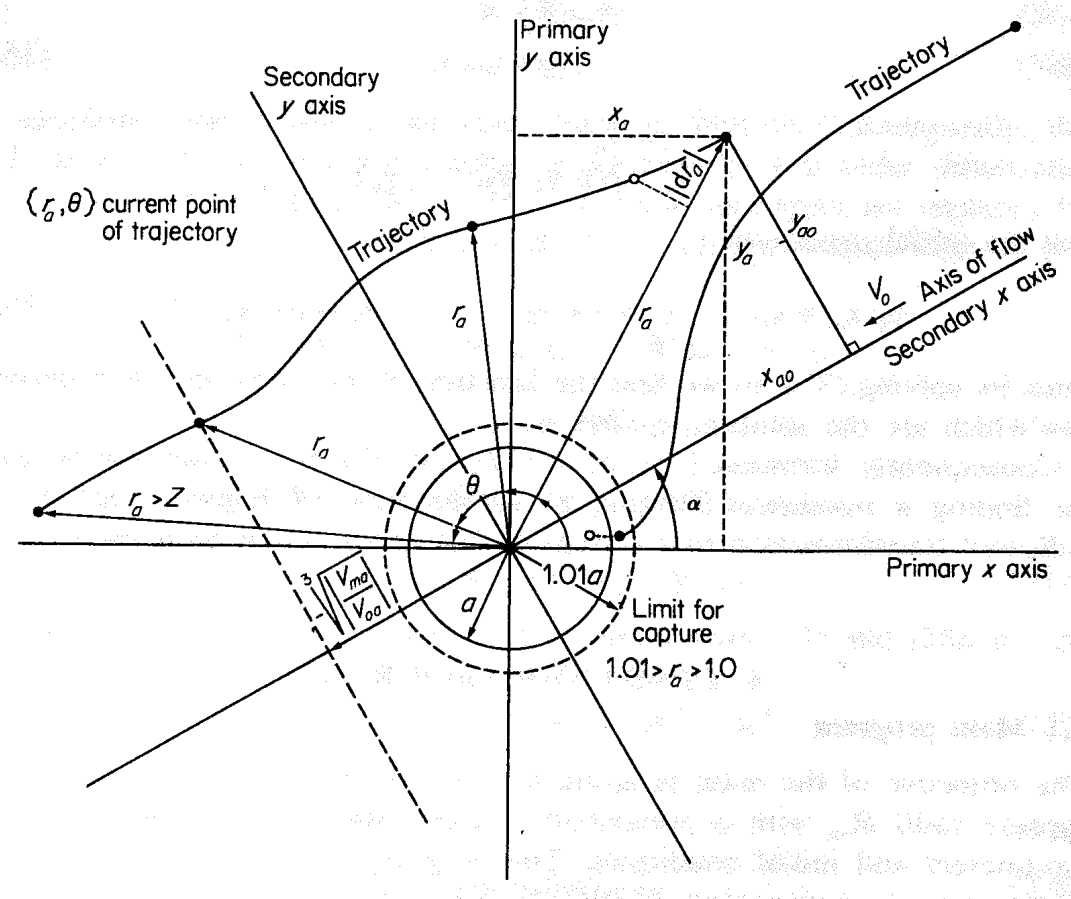

Figure 3. Definition of the primary and secondary frame of coordinates and the limiting conditions of capture and escape

later (by subroutines) in plane polar coordinates, where the iteration takes place;

VMA—the magnetic velocity V_{ma};

VOA—the fluid velocity V_{0a};

AK—the constant $K = M_s/2H_0$;

DTO—the time step length (a good empirical choice is DTO = $1/(10\ V_{0a})$), DTO is converted to the variable DT which can be adjusted during the iteration in subroutines;

E—the stipulated error (e.g. $E = 0.001$) of the Admas–Moulton predictor–corrector method.

Or

(b) if the XSECT subroutine has been chosen:
VMA, VOA, AK, DTO, ALPHA, XAO;

YLA and YHA—the lower and upper estimate of the y-coordinate (in the secondary frame) of a point lying on the critical curve.

The output data are:

(a) if either the RK or AM subroutine has been chosen:
AK, VMA, VOA, VMA/VOA, ALPHA, XAO, YAO;

X and Y—the x–y coordinates of the trajectory points in the primary frame of reference;

V—the velocity of the particle at each trajectory point;

DAR and DIT—the radial and angular components, dr_a/dt and $d\theta/dt$, of the velocity at each point;

DEET—the time step length dt between the points;

(b) if the XSECT subroutine has been chosen:
ITERATIONS and then AK, VMA, VOA, VMA/VOA, ALPHA;

XC—the x-coordinate (in the secondary frame) corresponding to the capture radius R_{ca} on the critical curve;

YC—the capture radius R_{ca}.

The flow chart of the MASTER section is shown in Figure 4.

The subroutine FUNCTN contains the equations of motion in the form of (19a, b).

The subroutines RK and AM each transfer the input parameters and the starting point from the MASTER section, compute one trajectory, return it to the MASTER section (to be printed out), and receive a new set of initial conditions to calculate the next trajectory.

The RK and AM subroutines use the following limiting conditions:

(i) the particle is captured $\leftrightarrow$ $1.0 < r_a < 1.01$;
(ii) the particle is beyond the range of interest $\leftrightarrow$ $r_a > Z = \max(14.2, r_{a0} + 0.2)$;
(iii) the impenetrability of the wire is violated $\leftrightarrow$ $r_a < 1.0$;
(iv) the overall step limit is violated $\leftrightarrow$ $|dr_a| > 0.1$.

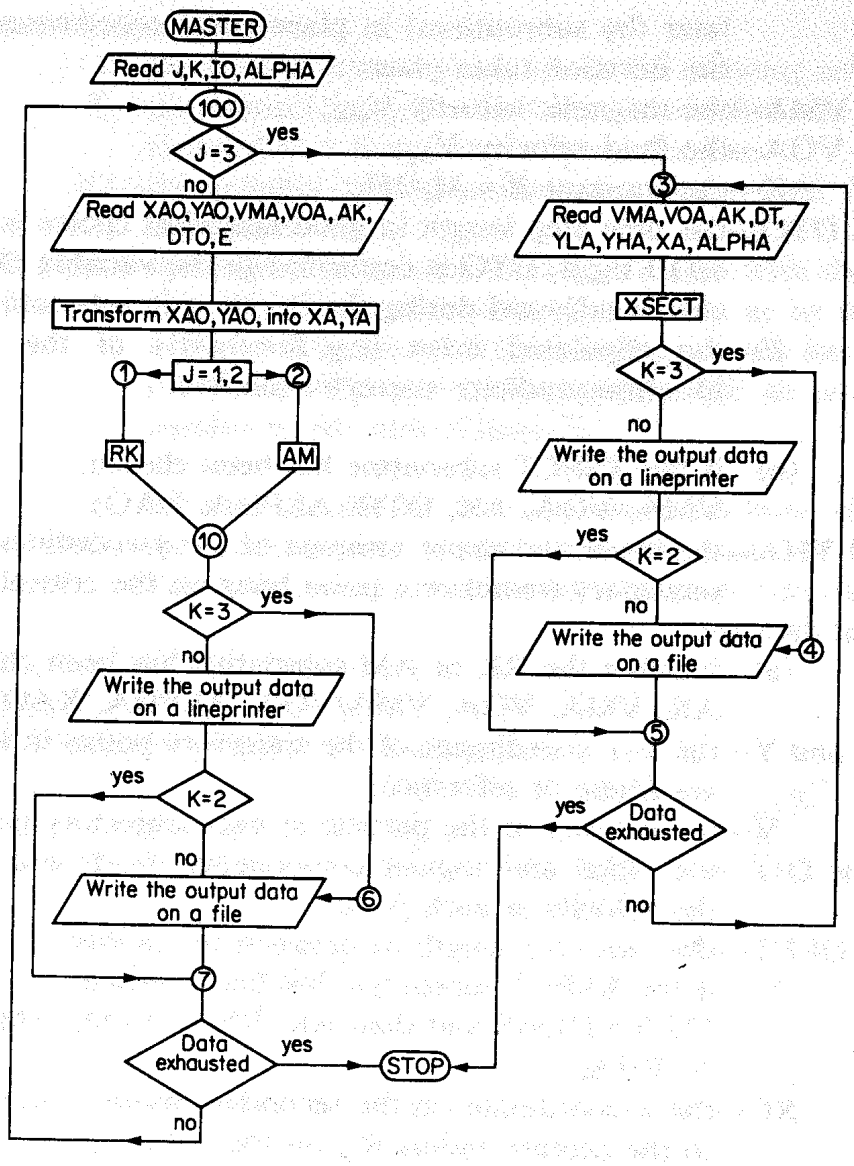

Figure 4. Flow chart of the MASTER section

If the condition (i) or (ii) is satisfied the control is returned to the MASTER section; if (iii) or (iv) takes place the step length DT is cut down.

The RK subroutine is based on the Runge–Kutta method as expressed by (32) and (33a, b, c, d). The AM subroutine uses the Runger–Kutta method as a starter and the Adams–Moulton method, given by (31a, b) as the main procedure. The role of the starter is not limited only to the initial point. After every cut in the step length DT the execution process is reversed to the Runge–Kutta method to provide four equally spaced points which are necessary for the action of the main predictor–corrector procedure. The process of execution in both subroutines, RK and AM, is apparent from the flow charts, which are shown in Figures 5 and 6, respectively.

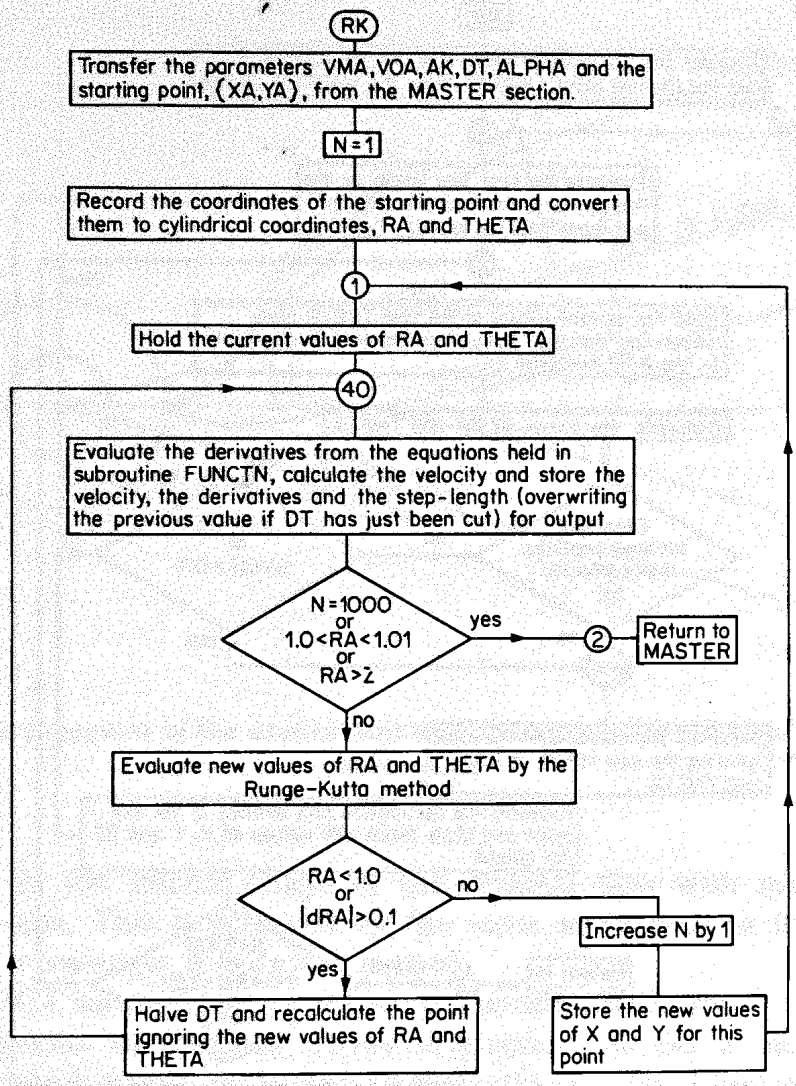

Figure 5. Flow chart of the RK subroutine

The XSECT subroutine calculates the capture radius R_{ca}. Again, the input data are transferred from the MASTER section, value of R_{ca} is computed and returned with iterations to be printed out. A new set of input data is transferred and the cycle repeated.

Before describing the flow of control in XSECT we have to consider a few points of a general nature.

It is apparent from equations (11a, b), (15a, b) and (17a, b) that the influence which the wire has upon the motion of the particle falls off with the distance r_a. Thus, beyond a certain region, the dimensions of which increases with $|V_{ma}/V_{0a}|$, the effect of the wire can be neglected and the trajectories are essentially parallel to the direction of the fluid flow (i.e. to